Insertion of Noble Gas Atoms into Cyanoacetylene: An ab Initio and Matrix Isolation Study

Leonid Khriachtchev,*,† Antti Lignell,† Hanna Tanskanen,† Jan Lundell,† Harri Kiljunen,‡ and Markku Räsänen†

Department of Chemistry, and VERIFIN, P.O. Box 55, FIN-00014 University of Helsinki, Finland

Received: June 15, 2006; In Final Form: August 18, 2006

A computational and experimental matrix isolation study of insertion of noble gas atoms into cyanoacetylene (HCCCN) is presented. Twelve novel noble gas insertion compounds are found to be kinetically stable at the MP2 level of theory, including four molecules with argon. The first group of the computationally studied molecules belongs to noble gas hydrides (HNgCCCN and HNgCCNC), and we found their stability for Ng = Ar, Kr, and Xe. The HNgCCCN compounds with Kr and Xe have similar stability to that of previously reported HKrCN and HXeCN. The HArCCCN molecule seems to have a weaker H−Ar bond than in the previously identified HArF molecule. The HNgCCNC molecules are less stable than the HNgCCCN isomers for all noble gas atoms. The second group of the computational insertion compounds, HCCNgCN and HCCNgNC, are of a different type, and they also are kinetically stable for Ng = Ar, Kr, and Xe. Our photolysis and annealing experiments with low-temperature cyanoacetylene/Ng (Ng = Ar, Kr, and Xe) matrixes evidence the formation of two noble gas hydrides for Ng = Kr and Xe, with the strongest IR absorption bands at 1492.1 and 1624.5 cm^{-1}, and two additional absorption modes for each species are found. The computational spectra of HKrCCCN and HXeCCCN fit most closely the experimental data, which is the basis for our assignment. The obtained species absorb at quite similar frequencies as the known HKrCN and HXeCN molecules, which is in agreement with the theoretical predictions. No strong candidates for an Ar compound are observed in the IR absorption spectra. As an important side product of this work, the data obtained in long-term decay of $KrHKr^+$ cations suggest a tentative assignment for the CCCN radical.

Introduction

Since Bartlett's discovery of the first Xe-containing molecule in 1962,[1] a large number of neutral ground-state species containing chemically bound noble gas (Ng) atoms have been analyzed and prepared. The vast majority of these molecules are xenon compounds.[2] Far fewer compounds of krypton have been synthesized.[3,4] Only one Ar-containing molecule (HArF) has been reported,[5] and no neutral Ne and He chemically bound species exist. Some theoretical predictions can be mentioned in this respect. As far as no good candidates have been found for Ne-containing molecules, the situation with He looks a bit more promising after Wang predicted that HHeF is a stable structure.[6] The later studies of this hypothetical molecule showed that its stability might be strongly limited by tunneling-induced decomposition, and some ways to overcome this problem have been suggested.[7−9] A few predictions for neutral Ar compounds are known, for instance, HArO, FArCCH, $FArSiF_3$, FArCu, and FArAg.[10−13] This short overview shows that the search for novel noble gas compounds, especially involving the lighter atoms (Ar, Ne, and He), is very challenging.

The synthesized HArF molecule belongs to a family of noble gas hydrides with the general formula HNgY (Ng = noble gas atom and Y = electronegative fragment).[14,15] Twenty molecules of this family has been synthesized and characterized to date. The first identified species were HXeCl, HXeBr, HXeI, and HKrCl,[16] and the latest examples, in addition to HArF,[5,17,18] are HKrF,[19] a noble gas open-shell species HXeO,[10] and organo noble gas insertion molecules prepared from acetylene and diacetylene.[20−24] The developed preparation procedure combines UV photolysis of HY precursors in a low-temperature noble gas matrix and thermal mobilization of the photogenerated hydrogen atoms.[14,15] Most of the relevant studies have been performed in noble gas matrixes; however, some of these HNgY molecules were reported in noble gas clusters in the gas phase.[25,26]

The preparation of HNgCCH and $HNgC_4H$ (Ng = Kr and Xe) suggests a general way for insertion of Ng atoms into the H−C≡ group.[20−24] The corresponding compounds with Ar do not show reliable computational stability, and they did not appear in the experiments. $HNgC_4H$ (Ng = Kr and Xe) seems to be more strongly bound than HNgCCH, at least computationally, and this was attributed to the larger electron affinity of C_4H than that of CCH.[23] In this situation, cyanoacetylene (HCCCN) looks like another promising candidate for insertion of noble gas atoms into the H−C bond. Possible insertion of Ng atoms into other bonds on this molecule is also interesting. Cyanoacetylene and its photolysis products are important, in particular, for Titan's atmosphere and have been studied both experimentally and theoretically.[27−32] Despite extensive efforts, the vibrational assignment of many related species is still lacking; for instance, the IR absorption spectrum of CCCN radical has not been reported to our knowledge.

In the present work, we study computationally and experimentally insertion of noble gas atoms into cyanoacetylene. Kinetic stability of a number of novel insertion compounds is

* Corresponding author. E-mail: leonid.khriachtchev@helsinki.fi.
† Department of Chemistry.
‡ VERIFIN.

10.1021/jp063731f CCC: $33.50 © 2006 American Chemical Society
Published on Web 10/04/2006

computationally found including four molecules with argon. In the experiments, we see evidence of two molecules containing krypton and xenon ($HKrC_3N$ and $HXeC_3N$) but no indication for argon compounds. The assignment of these and other related species is discussed.

Computations

Computational Details. In this work, we use both harmonic and anharmonic computational methods. The harmonic computations were carried out with the GAUSSIAN03 package of computer codes.[33] The electron correlation method was the second-order Møller−Plesset perturbation theory (MP2). The standard split valence basis set 6-311++G(*2d*,*2p*) was used to describe all atoms except Xe. For Xe atoms, LaJohn effective core potential (LJ18) combined with a valence shell optimized by Runeberg and Pyykkö was employed.[34] The Berny algorithm with tight convergence criteria was used for geometry optimization. For the complexes, the interaction energy is found as a difference between energies of the complex and the monomers, taking into account the basis set superposition error (BSSE) correction. The charge distributions were obtained with natural population analysis. Similar computational approaches have been used for other HNgY molecules and their complexes previously.[9,35,36]

The anharmonic computations on Kr-containing molecules were performed with the vibrational self-consistent field (VSCF) method and its extensions by corrections via the second-order perturbation theory.[37−40] This correlation-corrected VSCF (CC-VSCF) method is used to calculate the vibrational wave functions and energies, and only interactions between pairs of normal modes were included in the calculations. Each pair of normal modes was pictured with an 8×8 potential surface grid, and the normal mode couplings were evaluated by ab initio calculations over this grid. The CC-VSCF method is based on nondegenerate perturbation theory that can suffer from near-degeneracy problems. Especially in the case of HKrCCCN and HKrCCNC this could be a substantial risk, and therefore we used a degenerate perturbation theory variant of the CC-VSCF method, i.e., the VCI-VSCF method. The VCI stands for virtual configuration interaction solver, where the vibrational level energies are obtained in a valence space consisting of the ground state and both singly and doubly excited vibrational levels.[41] All anharmonic calculations based on the VSCF method were performed with the GAMESS (version R4, 2004) electronic structure program.[42] All anharmonic ab initio calculations employed the MP2(full) electronic structure theory. The C, N, and H atoms were described by the cc-pVDZ all electron basis set, whereas for krypton the cc-pVDZ-PP basis set was used.[43] The molecular structures were reoptimized in GAMESS with tight convergence criteria before employing the anharmonic calculations. The anharmonic computational approach has been previously applied for other HNgY molecules as a compromise between computational task and accuracy.[44,45]

The computations of the radical species were performed at the B3LYP/aug-cc-pVDZ level of theory in order to assess if such open-shell species are stable and thereafter to estimate the effect of the ^{15}N isotopic substitution. In principle, single-reference wave function methods such as MP2 seem to be unsuitable for these species, and therefore we have followed the path employing density functional theory for the open-shell species.

HNgCCCN, HNgCCNC, HCCNgCN, and HCCNgNC (Ng = Ar, Kr, Xe), Harmonic Approximation (MP2/6-311++G(*2d*,*2p*)). The insertion of noble gas atoms was computationally achieved into H−C, C−C, and C−N bonds of HCCCN and HCCNC (see Figure 1). True energy minima were obtained for Ng = Ar, Kr, Xe. For Ng = Ne and He, the corresponding species are unstable. The computational structural parameters, strongest absorptions, and dissociation energies are collected in Table 1. The obtained bond lengths between noble gas and other atoms (H, C, and N) are much shorter than the corresponding van der Waals distances, suggesting real chemical bonding. The calculated changes of the other remaining bonds with respect to the HCCCN and HCCNC monomers are minor. For reference, the bond distances in HCCCN at this level of theory are 1.0611, 1.2154, 1.3742, and 1.1751 Å, and the values for HCCNC are 1.0598, 1.2103, 1.3166, and 1.186 Å. The stabilization energies of the compounds with respect to the dissociation asymptotes increase from Ng = Ar to Kr and Xe for all calculated molecules. These noble gas molecules are metastable with respect to the Ng + HC_3N energy. In fact, HNgCCCN molecules are higher in energy than the HCCCN + Ng asymptote by 6.4, 5.6, and 4.3 eV for Ng = Ar, Kr, and Xe, respectively. The decomposition of the HNgY molecules to the ground-state HY + Ng products is, as a rule, protected by a relatively high bending barrier.[15] We scanned the potential energy surface of HNgCCCN with respect to the H−Ng−C bending coordinate. This yielded bending barriers of 1.0 and 1.3 eV for Ng = Ar and Kr, respectively, protecting the HNgCCCN molecules from the spontaneous decomposition to the HCCCN + Ng fragments.

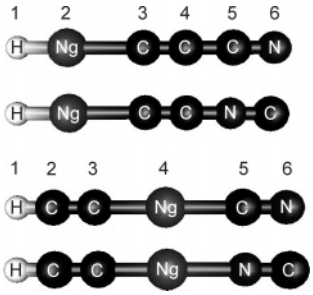

Figure 1. Computational geometries and labeling of atoms in the noble gas compounds. The distances are given in Table 1.

For insertion of an Ng atom into the H−C bond (HNgCCCN and HNgCCNC), the vibrational spectrum is dominated by the very strong H−Ng stretching absorption. The vibrational modes presented in Table 1 mainly originate from the C≡N (ω_1), H−Ng (ω_2), and C−C (ω_3) stretching vibrations. The species are of a charge-transfer character with the positive charge on the (H−Ng) part, similarly to other HNgY molecules.[14,15] The obtained frequencies for the H−Kr and H−Xe stretching modes are close to the results of the harmonic calculations on relatively strongly bound noble gas hydrides. For comparison, we performed calculations on previously identified HXeCN and HKrCN molecules at the present level of theory and found 1820.7 and 1774.9 cm^{-1} for the H−Xe and H−Kr stretching frequencies. The H−Ng bond lengths in HNgCCCN and HNgCN species are also reasonably similar (1.7308 and 1.7180 Å for Ng = Xe and 1.5405 and 1.5229 Å for Ng = Kr, respectively) as well as the charge separations (for instance, +0.660 and +0.636 elementary charges on the H−Kr part of HKrCN and HKrCCCN, respectively). The dissociation energies for HXeCN and HKrCN at the used level of theory are 2.152 and 0.891 eV. On the basis of this comparison, the experimental preparation of HXeCCCN and HKrCCCN is very probable. The Ar compound HArCCCN has a quite lower H−Ar stretching frequency (1555.5 cm^{-1}) than the value of previously identified HArF [2149 cm^{-1} at the MP2/6-311++G(*2d*,*2p*) level of

TABLE 1: Computed Bond Lengths (angstroms), Strongest Absorptions (cm^{-1}), and Absorption Intensities (km/mol, in Parentheses) of Various Insertion Molecules[a]

	HNgCCCN	HNgCCNC	HCCNgCN	HCCNgNC
1−2	1.4045	1.4265	1.0619	1.0616
	1.5405	1.5488	1.0615	1.0612
	1.7308	1.7327	1.0619	1.0616
2−3	2.2359	2.2197	1.2206	1.2114
	2.2973	2.2903	1.218	1.212
	2.3418	2.3376	1.2209	1.2177
3−4	1.2356	1.2308	2.066	1.8124
	1.2354	1.2311	2.0574	1.9239
	1.2350	1.2309	2.1617	2.0919
4−5	1.3718	1.3182	2.0839	2.0753
	1.3715	1.3181	2.1679	2.1636
	1.3713	1.317	2.2572	2.2161
5−6	1.1770	1.1879	1.1781	1.1883
	1.1772	1.1877	1.1765	1.1873
	1.1772	1.1878	1.1764	1.1873
ω_1	2183.4 (34)	2164.9 (7)	3463.1 (57)	3470.2 (107)
	2180.9 (29)	2165.7 (12)	3468.3 (67)	3474.4 (94)
	2178 (15)	2168.6 (35)	3463.3 (69)	3467.2 (76)
ω_2	1555.3 (4783)	1426.4 (5122)	2023.7 (128)	1997.4 (498)
	1692.3 (2606)	1651.8 (2637)	2048.6 (128)	2010.3 (394)
	1777.4 (1217)	1775.2 (1189)	2054.2 (107)	2014.9 (364)
ω_3	908 (253)	961 (129)	633.8 (81)	676.8 (74)
	912.3 (163)	962.8 (78)	674.3 (82)	701.6 (75)
	918.7 (125)	970.7 (65)	667.6 (82)	669.0 (79)
binding energy	−0.68	−0.11	−1.07	−0.34
	−1.51	−0.94	−2.08	−1.52
	−2.80	−2.23	−3.76	−3.29

[a] The calculations are performed at the MP2/6-311++G(*2d*,*2p*) level of theory. The atoms are numbered as shown in Figure 1. The upper, middle, and lower values in a cell correspond to Ng = Ar, Kr, and Xe. Also presented is the binding energy (in eV) of the species with respect to the H+Ng+C_3N and HCC+Ng+CN asymptotes. The data are presented for ^{14}N isotope.

theory], and the H−Ar bond length (1.4045 Å) is substantially longer than the 1.326 Å reported for HArF.[35] It follows that the computational H−Ar bond in HArCCCN is relatively weak. On the other hand, HArCCCN is quite stable compared to that of the recently carefully calculated $HArC_4H$ with the computational stabilization energy of 0.45 eV, the H−Ar distance of 1.495 Å, and the H−Ar stretching frequency of 1136 cm^{-1}.[46] Our computations indicate a lower stability of the HNgCCNC isomers as compared to that of HNgCCCN (by ∼0.55 eV); nevertheless, the HNgCCNC species with Ng = Kr and Xe are also promising candidates for experimental preparation.

The HCCNgCN and HCCNgNC species exhibit a different class of noble gas molecules because no H−Ng bond is present here. Similar noble gas species without a H−Ng bond were predicted earlier (for instance, HCCArF and FXeSiF);[11,12] however, they have not been prepared experimentally. We found computational stability of all HCCNgCN and HCCNgNC (Ng = Ar, Kr, and Xe) molecules. The Ng atoms are charged positively in these structures (for instance, by +0.965 elementary charge for HCCXeCN), and the HCC and NC parts are negatively charged (by −0.430 and −0.535 for HCCXeCN). As a trend, the charge separation is stronger for HCCNgNC molecules than for HCCNgCN and weaker for Ng = Kr and Ar than for Ng = Xe. The obtained Ng−C and Ng−N distances are quite short. For instance, the computational C−Xe distances in HCCXeCN are 2.1617 and 2.2572 Å, whereas it is 2.3690 Å in HXeCN. To our knowledge, the HCCArNC molecule represents the first computational result on the stable Ar−N bond in a neutral compound (distance 2.0753 Å).

Kr···HKrCCCN and Kr···HKrCCNC Complexes. We investigated computationally the 1:1 interaction between the Kr-containing hydrides with Kr atoms, which is relevant to our experimental matrix isolation work. Three structures were found for the complex with all real vibrational frequencies, indicating that the energy minima were true (see Figure 2). Two of these structures (complexes A and B) are linear and quasi-linear arrangements where the Kr atom interacts with the molecule from the opposite ends. One structure (complex C) is bent. Similar structures were previously found for the Xe···HXeBr complex.[36] The interaction somewhat changes the H−Kr and Kr−C distances with respect to those of the monomeric species, and the shortest H−Kr distance is obtained for complex A (linear). The shortening on the H−Kr bond distance correlates with the increase of the (H−Kr) positive charge.

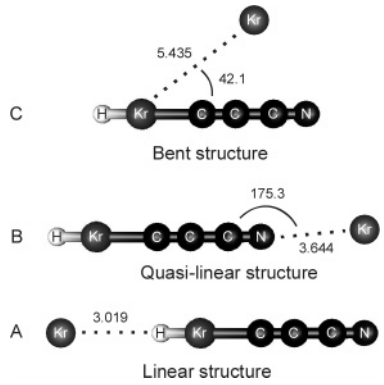

Figure 2. Computational geometries of the Kr···HKrCCCN and Kr···HKrCCNC complexes. The figure applies to the Kr···HKrCCCN isomer. The values for the Kr···HKrCCNC isomer are the following. The intermolecular distance is 3.061 Å for linear, 3.908 Å for quasi-linear, and 5.586 Å for bent structures, and the angle is 175.2° for quasi-linear and 41.0° for bent structures.

The vibrational and energetic properties of the optimized complex structures are given in Table 2. The complexation

TABLE 2: Computed Vibrational Frequencies and Interaction Energies of Kr-Containing Hydrides Complexed with Kr Atoms[a]

	HKrCCCN				HKrCCNC			
	Mon.	A	B	C	Mon.	A	B	C
ω_1	2180.9	2180.0	2179.3	2179.4	2165.7	2163.5	2165.0	2163.6
ω_2	1692.3	1734.0	1696.3	1694.0	1651.8	1687.8	1656.8	1655.6
ω_3	912.3	911.3	912.8	912.5	962.8	961.3	963.1	963.0
E (Int.)		−143.6	−144.3	−262.5		−80.2	−44.5	−213.3

[a] The interaction energies are BSSE corrected (in cm^{-1}). The vibrational frequencies (for the strongest absorptions) are in cm^{-1}. The mode notations (ω_1, ω_2, and ω_3) are the same as in Table 1. The data are presented for the ^{14}N isotope.

TABLE 3: Anharmonic Vibrational Spectra (in cm^{-1}) of $HKrC_3N$ Isomers with the MP2(full)/cc-pVDZ-PP Level of Theory[a]

molecule	mode	harmonic	diagonal	CC-VSCF	intensity	VCI-VSCF
HKrCCCN	ω_1	2222.2	2177.1	2139.1	17.1	2142.3
		2222.1	2177.0	2138.4	25.1	2141.8
		2211.1	2166.9	2128.1	16.6	2131.7
	ω_2	1761.9	1605.0	1576.8	2690.4	1559.9
		1252.9	1164.5	1150.2	1364.2	1140.1
		1761.9	1605.0	1576.7	2690.8	1559.7
	ω_3	930.4	909.3	904.8	148.4	908.7
		929.3	908.1	903.8	181.4	907.6
		920.0	899.1	895.3	150.2	899.0
HKrCCNC	ω_1	2189.3	2146.1	2113.1	2.4	2111.5
		2189.3	2146.1	2112.1	2.3	2111.0
		2171.8	2128.8	2097.1	1.5	2093.9
	ω_2	1739.3	1590.7	1561.6	2608.2	1547.4
		1236.3	1151.3	1137.7	1355.5	1128.8
		1739.3	1590.8	1561.5	2608.7	1547.3
	ω_3	974.1	952.1	838.4	67.7	944.1
		973.6	951.6	847.0	86.5	943.4
		970.4	948.2	545.4	69.0	940.3
HKrNCCC nonlinear[b]	ω_1	2271.9	2228.2	2128.2	139.3	2145.8
		2188.0	2158.1	2106.3	1523.2	2113.8
		2267.1	2219.9	2119.9	169.6	2136.0
	ω_2	2098.4	2043.0	1915.7	4274.8	1924.6
		1548.8	1422.6	1406.0	1754.8	1392.3
		2094.6	2043.8	1906.5	4187.8	1927.0
	ω_3	935.5	914.1	906.5	10.2	905.7
		935.1	913.6	906.4	10.6	905.7
		922.9	901.9	894.7	10.1	894.1
HKrCNCC nonlinear[c,d]	ω_1	2149.6	2021.2	1915.8	1045.8	1962.7
		2000.2	1993.3	1924.1	1687.6	1977.1
		2147.1	2006.7	1902.2	1234.9	1942.1
	ω_2	1976.2	1972.5	1865.7	3235.4	1932.3
		1508.4	1396.2	1354.4	1701.4	1345.6
		1959.9	1949.0	1854.2	2822.0	1916.1
	ω_3	971.8	949.4	937.6	33.2	943.6
		971.3	948.9	935.1	35.8	941.6
		966.2	944.1	932.2	27.9	939.0

[a] The absorption intensity is in km/mol. The three frequency values in a cell correspond to the H/^{14}N, D/^{14}N, and H/^{15}N isotope analogs. The mode notations (ω_1, ω_2, and ω_3) are the same as in Tables 1 and 2. [b] HKrNCCC in linear configuration is unstable with imaginary frequencies in harmonic calculations. The bent structure has a Kr−N−C angle of 116.0°. [c] HKrCNCC in linear configuration is unstable with imaginary frequencies in harmonic calculations. The bent structure has a Kr−C−N angle of 152.1°. [d] HKrCNCC (nonlinear) has another strong mode (harmonic 1877.05 cm^{-1}, intensity 185.7 km/mol, anharmonic 1808.5 cm^{-1}).

increases the H−Kr stretching frequency for all the complex structures with respect to that of the monomer, especially for complex A. The blue shift of this mode seems to be a normal case for the HNgY complexes;[9,35,36,47] however, the red shift has been computationally found to be possible as well.[36,48] The increase of the vibrational frequency correlates with shortening of the H−Kr bond similarly to the previous studies on HNgY complexes. The complexation effect is weaker for the two other characteristic vibrational modes (ω_1 and ω_3). Complexes A and B were found to have similar interaction energies, and complex C exhibits a stronger interaction for both molecules.

$HKrC_3N$ Isomers, CC-VSCF Method. We considered Kr-containing hydrides using anharmonic calculations, and the results are presented in Table 3. The noble gas hydrides are highly anharmonic species, and the anharmonic corrections on their vibrational spectra can be quite large.[44,45] Thus, it was important to compare the harmonic and anharmonic spectra in order to test the quality of the harmonic results. First, the harmonic results obtained with the MP2(full)/cc-pVDZ-PP level of theory used in these anharmonic computations are close to the results obtained above with the more time-consuming MP2(full)/6-311++G(*2d*,*2p*) method (see Table 1). Second, the

TABLE 4: Computational Characteristic IR Absorption Bands (in cm^{-1}, the Intensity in km/mol in Parentheses) of Related Species[a]

	HCCCN	HCCNC	$CCCN^-$	$CCNC^-$	CN^-	CCNC (^{2}D)[b]	CCNC (^{4}D)[b]	CCCN
^{14}N	3475.6 (81)	3590.2 (94)	2129.1 (383)	2035.1 (254)	1984.5 (3)	2064.0 (463)	1856.7 (206)	2128.8 (211)
	2207.3 (6)	2229.3 (42)	1904.8 (14)	1896.3 (16)		1766.8 (93)	1250.2 (8)	1679.5 (556)
	2026.6 (3)	2021.8 (42)	870.1 (12)	884.9 (7)		949.9 (4)	935.5 (27)	909.1 (6)
	662.6 (40)	635.7 (43)						
	654.3 (39)	627.9 (43)						
^{15}N	3475.5 (81)	3490.2 (94)	2115.0 (386)	2009.6 (262)	1953.8 (2)	2024.3 (454)	1823.4 (196)	2103.4 (217)
	2196.7 (6)	2211.6 (33)	1894.1 (7)	1884.5 (4)		1766.3 (88)	1248.7 (8)	1677.5 (548)
	2012.1 (2)	1998.7 (48)	859.6 (12)	879.9 (8)		945.5 (3)	931.7 (27)	899.4 (5)
	662.6 (40)	635.5 (43)						
	654.4 (39)	627.8 (43)						

[a] The first five closed-shell species are calculated at the MP2/6-311++G(*2d*,*2p*) level of harmonic theory. CCNC and CCCN radicals are calculated with the B3LYP/aug-cc-pVDZ harmonic method. The low-frequency bands (<500 cm^{-1}) are not shown. [b] CCNC (^{2}D) is a quasi-linear structure with a C−C−N angle of 164.4°; CCNC (^{4}D) is an excited radical having a bent structure with a C−C−N angle of 124.1°.

main effect of anharmonicity is a decrease of the H−Kr stretching frequency, from 1762 to 1560 cm^{-1} for HKrCCCN and from 1739 to 1547 cm^{-1} for HKrCCNC. The effect of anharmonicity on other modes is weaker but also essential (e.g., from 2222 to 2142 cm^{-1} for ω_1 of HKrCCCN).

In this part of computational work, we found two additional isomers of $HKrC_3N$. While linear HKrCNCC and HKrNCCC structures are computationally unstable, their bent configurations feature local stability. Their vibrational spectrum is characterized by quite higher H−Kr stretching frequencies compared with those of the two first species (by about 400 cm^{-1} in the anharmonic approximation). HKrCNCC (nonlinear) computationally exhibits an additional strong band at 1808 cm^{-1}.

Table 3 shows the vibrational frequencies of these molecules upon D/H and ^{15}N/^{14}N isotope substitutions. The main deuteration effect is the normal downshift of the strongest absorption involving hydrogen (mode ω_2). The other absorption frequencies change less extensively upon deuteration. For instance, the ω_1 mode frequency (at ∼2142 cm^{-1}) of HKrCCCN changes upon deuteration by −0.5 cm^{-1}. For the nonlinear molecules, deuteration changes essentially the ω_1 mode frequency (by −32 cm^{-1} for HKrNCCC). The ^{15}N substitution essentially affects the ω_1 and ω_3 mode frequencies, but the change of the H−Kr stretching frequency is minor.

Related Species. A number of species (HCCCN, HCCNC, $CCCN^-$, $CCNC^-$, CN^-, CCNC, CCCN) were additionally computed because they are relevant to the present experimental work and aid the assignments. The main purpose of these computations is to compare spectroscopic data for ^{14}N- and ^{15}N-labeled species (see Table 4). We report the B3LYP results on the open-shell species because the corresponding MP2 results are not satisfactory.

Experimental Section

Experimental Details. The HCCCN/Ng (∼1/1000) solid mixtures were studied in a closed-cycle helium cryostat (APD, DE 202A) at temperatures down to 8 K. The matrixes (∼100 μm thick) were deposited onto a cold CsI substrate from the gaseous mixture, the deposition temperatures being ∼10, 20, and 30 K for Ar, Kr, and Xe samples, respectively. The 193 nm radiation of an excimer laser (MSX-250, MPB, pulse energy density ∼10 mJ/cm^2) was typically used to photolyze the samples. In some experiments, radiation of an optical parametric oscillator (Sunlite with FX1 UV frequency extension) and an Ar-ion laser (488 nm, Omnichrome 543-AP) were employed. The IR absorption spectra in the 4000−400 cm^{-1} region were recorded with a Nicolet 60 SX FTIR spectrometer using a resolution of 1 cm^{-1}.

TABLE 5: Experimental IR Absorption Bands (in cm^{-1}) of the HC_3N Isomers for Various Matrices (Ar, Kr, Xe) and Isotope Substitutions (H/D and ^{14}N/^{15}N)

Ar/H/^{14}N	Kr/H/^{14}N	Xe/H/^{14}N	Kr/D/^{14}N	Kr/H/^{15}N	assignment[a]
3315	3304, 3305	3295, 3297	2594	3303	HCCCN
2269	2265	2263	2242	2249	
2076	2073	2070	1962	2062	
1318	1313, 1316	1311, 1314	1017, 1042	1313,1316	
666	664, 667	663, 666	522	664, 667	
3328	3317	3308	2604	3316	HCCNC
2213	2208	2204	2146	2193	
2033	2030	2027	1958	2006	
3562	3551	3549?	2686	3542	HNCCC
2205	2200	2196	2157	2191	
1905	1903	1901	1878	1894	
2102	2098	2096		2062?	HCNCC

[a] Using data of ref 30.

Cyanoacetylene (HCCCN) and its D and ^{15}N isotopic analogues were prepared as follows. Cyanoacetylene was synthesized by the method of Melamed and Feit.[49] Propiolamide (0.3 g, 4.35 mmol, Acme Bioscience Inc.) was heated together with phosphorus pentoxide (0.9 g, Aldrich, >98%). A helium (AGA) stream (approximately 10 mL/min) was passed through the reaction mixture, and the formed cyanoacetylene was collected from the helium stream in a trap, which was cooled by liquid nitrogen. To prepare deuterated cyanoacetylene, cyanoacetylene-containing carrier gas (helium) was passed through 10 mL of D_2O (Aldrich, >99%), dried with anhydrous $CaCl_2$, and collected as previously described. To prepare ^{15}N-labeled cyanoacetylene, we first synthesized ^{15}N propiolamide by the method of Hay et al.[50] A 6 M $^{15}NH_4OH$ (ICON isotopes, 98%) aqueous solution was cooled to −10 °C, and ethyl propiolate (EGA-Chemie, 99%) was added slowly. The reaction mixture was warmed slowly to room temperature. The water was removed by azeotropic distillation with benzene in a Dean−Stark trap. ^{15}N-labeled cyanoacetylene was synthesized as described above using ^{15}N propiolamide.

Experimental Results. The deposited HCCCN/Ng samples are quite monomeric with respect to cyanoacetylene for all matrix materials. In Table 5, the IR absorption bands are presented for Ar, Kr, and Xe matrixes and for various isotope substitutions in a Kr matrix. The HCCCN absorption bands in an Ar matrix agree with the literature data,[28,30] and the data for Kr and Xe matrixes feature normal matrix shifts. The calculations (see Table 4) predict reasonably well the ^{15}N/^{14}N shift for this molecule.

UV radiation decomposes HCCCN molecules and produces numerous absorption bands. For 193 nm photolysis in an Ar

TABLE 6: Experimental IR Absorption Bands of the Photolysis and Annealing Products of HCCCN (in Addition to HCCCN Isomers) for Various Matrices (Ar, Kr, Xe) and Isotope Substitutions (H/D and $^{14}N/^{15}N$)

Ar/H/^{14}N	Kr/H/^{14}N	Xe/H/^{14}N	Kr/D/^{14}N	Kr/H/^{15}N	assignment/comment
1778	1764		1764	1754	C_2N^-[a]
558	552		552	550	correlates with the previous band[b]
1792 901	1781, 1776 898		1781, 1776 898	1779, 1776 890	C_2NC bent[a]
2023	2019		2019	1982	CN^-[a]
1461	1449		1449	1442	correlates with the previous band
2194	2190 2174? 2169?	2181 2171? 2157?	2190 2174? 2169?	2166 2151?	C_3N^-[a]
2090	2087	2082	2087	2085	C_2NC^-[a]
902	853, 1008, 1160, 1309	731,843, 954	606	853, 1008, 1160, 1309	$NgHNg^+$
2303 2079	2298 2076	2280 2066	2298 2076	2284 2066	CCCN annealing induced[c]

[a] Based on the assignment of ref 30 done in an Ar matrix. [b] This absorption fits a band of C_2N^-, which is computationally strong and locates at 551 cm^{-1} (scaled) (ref 30). [c] Our assignment for CCCN is tentative.

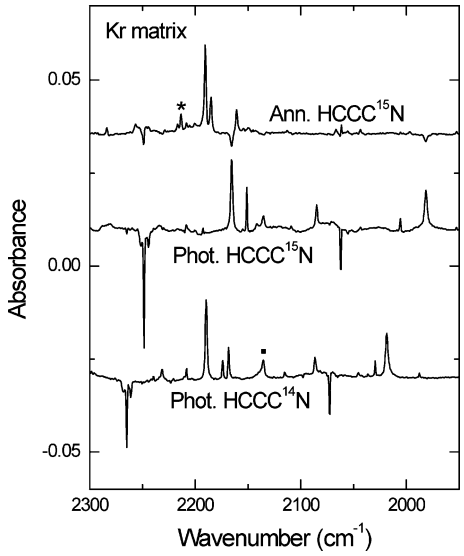

Figure 3. Photolysis and annealing of cyanoacetylene in a Kr matrix. Shown are (from bottom to top) the results of 193 nm photolysis for the ^{14}N- and ^{15}N-labeled cyanoacetylene and the result of annealing at 30 K of photolyzed matrixes with ^{15}N-labeled cyanoacetylene. The bands decreasing upon photolysis belong to cyanoacetylene. The band marked with an asterisk is assigned to the Kr hydride compound, and the band marked with a dot is from carbon monoxide. The presented spectra are difference spectra showing the result of photolysis or annealing.

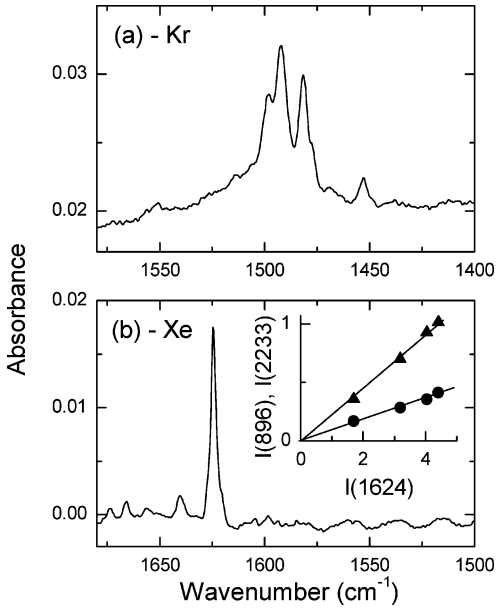

Figure 4. Spectra of (a) Kr and (b) Xe noble gas hydrides in the H−Ng stretching region. The spectra were obtained by 193 nm photolysis of cyanoacetylene in noble gas matrixes and annealing at 30 K (Kr) and 45 K (Xe). The inset in panel b shows the correlation of the main band at 1624.5 cm^{-1} with the weaker bands at 896 and 2233 cm^{-1} obtained by using photodissociation at 250 nm. The data points shown in the inset correspond to different durations of photodissociation.

matrix, most of these bands are found in the spectra reported by Guennoun et al. for VUV photolysis.[30] The results of $HCCC^{14}N$ and $HCCC^{15}N$ photolysis in a Kr matrix are presented by the two lower traces in Figure 3. The photolysis-induced absorption bands are presented in Tables 5 and 6 together with the literature assignments for an Ar matrix. The photolysis products are similar in Ar and Kr matrixes, but the situation changes in a Xe matrix. For example, no analogues to the bands assigned previously to CN^- and bent CCNC are seen in a photolyzed HCCCN/Xe matrix. The photolysis-induced formation of hydrogen-free species and $NgHNg^+$ cations show that hydrogen atoms can escape the parent cage and stabilize in the matrix at 8 K.[51]

Hydrogen atom mobility is activated upon annealing at ∼20 K in solid Ar, at 30 K in solid Kr, and at 40 K in solid Xe.[17,18,52−54] Accordingly, a number of absorption bands rise upon annealing evidencing reactions of mobile hydrogen atoms. One pronounced product of annealing is the HNCCC isomer (see Figure 3 and Table 5). The products shown in Figure 4 are specific for the matrix: we observe a bunch of bands around 1492 cm^{-1} in a Kr matrix and a strong single band at 1624.5 cm^{-1} in a Xe matrix, and no analogous bands were found in an Ar matrix. Upon deuteration, these bands shift down to 1108, 1105, and 1099 cm^{-1} in a Kr matrix and to 1177.7 cm^{-1} in a Xe matrix. Upon ^{15}N isotope substitution these bands are practically unchanged. These absorption bands are assigned to the H−Ng stretching modes of noble gas hydride molecules $HNgC_3N$ (Ng = Kr and Xe). The annealing-induced formation of HXeH (1166 and 1181 cm^{-1}) is observed in a Xe matrix.[14,15]

As a rule, the HNgY molecules quickly decompose upon irradiation with UV or visible light, which is due to their weak bonding and a large transition dipole moment to the repulsive

TABLE 7: IR Absorption Bands of the Annealing-Induced Noble Gas Species for Ng = Kr and Xe and Isotope Substitution (H/D and $^{14}N/^{15}N$)[a]

	$HKrC_3N$ in Kr matrix			$HXeC_3N$ in Xe matrix		
	Kr/H/^{14}N	Kr/D/^{14}N	Kr/H/^{15}N	Xe/H/^{14}N	Xe/D/^{14}N	Xe/H/^{15}N
ω_1	2230, 2234	2230, 2233	2213, 2217	2232	2232	2213, 2215
ω_2	1498, 1492, 1482, 1478, 1453?	1108, 1105, 1099	1498, 1492, 1482, 1478, 1453?	1624.5	1177.5	1624.5
ω_3	892, 894	890, 891	884, 885	896	898	893

[a] The mode notations (ω_1, ω_2, and ω_3) are the same as in Tables 1 and 3. Annealing in a Xe matrix also leads to HXeH (refs 14 and 15).

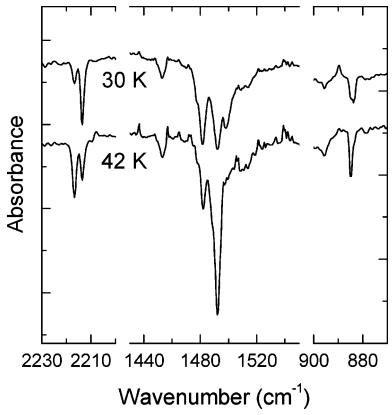

Figure 5. Decomposition of the Kr insertion compound $HKrC_3N$. The selective decomposition of the noble gas hydride was done with continuous wave radiation at 488 nm. Prior to photodissociation, the photolyzed HC_3N/Kr samples were annealed at 30 and 42 K as shown in the plot. Notice the change of the matrix site structure in the two spectra. The presented spectra are difference spectra showing the result of photodissociation.

excited states.[55,56] The efficient photodissociation can be used as a characteristic fingerprint of these molecules and aids identifications of weaker bands of the same species.[56] We irradiated the samples at various wavelengths (193, 250, and 488 nm) in order to identify other bands of the same noble gas species. As a result, additional bands are found to correlate with the strongest H−Ng stretching absorptions: the bands at 892, 894, 2230, and 2234 cm^{-1} correlate with the 1492 cm^{-1} band in a Kr matrix, and the bands at 896 and 2232 cm^{-1} correlate with the 1624 cm^{-1} band in a Xe matrix [see the inset in Figure 4b]. The bands observed at 896 and 2232 cm^{-1} in a Xe matrix are rather weak. These additional bands are sensitive to D/H and $^{15}N/^{14}N$ isotope substitution as shown in Table 7. It was also found that the annealing at higher temperatures (~40 K) synchronously modify the band structure of the Kr-containing species in all spectral regions, which is demonstrated in Figure 5.

Discussion

Assignment of $HNgC_3N$ (Ng = Kr and Xe). The assignment of the strongest IR absorption bands (mode ω_2) presented in Figure 4 and Table 7 to the H−Ng stretching vibration of noble gas hydrides is straightforward; however, the exact chemical formulas should be carefully discussed. These bands are sensitive to the matrix material (Kr and Xe), and no analogues are found in an Ar matrix. This behavior is similar to the observations on HNgCCH and $HNgC_4H$ (Ng = Kr and Xe) molecules prepared from acetylene and diacetylene and noble gas atoms.[20,22,23] The present species are formed at temperatures specific for thermal diffusion of hydrogen atoms in noble gas solids, which is the usual case for noble gas hydrides. Deuteration of cyanoacetylene leads to a proper downshift of the H−Ng stretching frequency with the H/D ratios of 1.349 and 1.380 for Ng = Kr and Xe, respectively. These annealing-induced bands are efficiently bleached by light, which is also characteristic for noble gas hydrides. The band fine structure of the Kr-containing molecule, which is most probably due to the matrix site effect, is very similar to that of the H−Kr stretching bands of HKrCCH and $HKrC_4H$.[22,23] We observed absorptions in three spectral regions for the $HNgC_3N$ molecules (see Table 7), and they are also the strongest bands in the computational vibrational spectrum (ω_1, ω_2, and ω_3 modes in our notations).

It is more difficult to distinguish the assignment between the HNgCCCN and HNgCCNC isomers. The computational H−Ng stretching frequencies of these species are quite similar and cannot be used for identification. However, the ω_1 and ω_3 bands (see Table 3) fit better the HNgCCCN isomer than HNgCCNC. For these modes, the difference of the anharmonic computational values from the experimental positions is −90 and +15 cm^{-1} for HKrCCCN and −130 and +51 cm^{-1} for HKrCCNC. For the harmonic theory (see Table 1), the corresponding computational mismatch is −42 and +11 cm^{-1} for HKrCCCN and −57 and +70 cm^{-1} for HKrCCNC. As a reference, the 2265 cm^{-1} experimental band of HCCCN in a Kr matrix was missed in the harmonic computations by a similar value of −58 cm^{-1} and the 2190 cm^{-1} experimental band of $CCCN^-$ by −61 cm^{-1}. The experimental integrated intensities of these modes ($\omega_1/\omega_2/\omega_3$ = 4/100/9) are closer to the computational values for HKrCCCN (1.1/100/6.3) than for HKrCCNC (0.23/100/1.5). The deuteration effect on the ω_1 and ω_3 bands is small for HNgCCCN and HNgCCNC both in experiment and theory. The anharmonic computational shifts for these modes upon ^{15}N isotope substitution are ca. −11 and −10 cm^{-1} for HKrCCCN and −18 and −4 cm^{-1} for HKrCCNC. In the experiments, these values are ca. −17 and −9 cm^{-1}, fitting both HKrCCCN and HKrCCNC. The computational spectra for other isomers presented in Table 3 (nonlinear HKrNCCC and HKrCNCC) disagree with the experimental data with respect to the ω_2 mode and some isotopic substitutions. Similar conclusions are valid for the case of Xe. The close positions of the ω_1 and ω_3 bands for the Kr and Xe compounds suggest the same isomeric structure. The annealing-induced formation of HNCCC is observed, which is consistent with the absence of HNgNCCC. On the other hand, the HCCCN concentration does not increase upon annealing, which is consistent with formation of HNgCCCN molecules. Similarly, in the experiments with HCN in a Kr matrix, annealing of the photolyzed matrix promoted formation of HKrCN and HNC.[57] The annealing-induced formation of HNCCC shows that CCCN radicals are present in the matrix in good amounts allowing formation of HNgCCCN (see also later). The HNgCCCN molecule is computationally lower in energy than HNgCCNC. Based on these arguments, we conclude that HNgCCCN (Ng = Kr and Xe) are the most probable candidates for the species presented in Table 7.

The possible formation of HNgCN molecules in these experiments should be discussed because their H−Ng stretching absorptions are close to the bands observed in the present study.[57] CN radicals can in principle be present after photolysis in some amounts even though their absorption bands are not observed. We repeated experiments with photolysis and annealing of HCN/Ng (Ng = Kr and Xe) matrixes described in detail in ref 57. The obtained H−Ng stretching absorptions of HNgCN (1497.8 cm^{-1} for HKrCN and 1623.7 cm^{-1} for HXeCN) are somewhat different from the values appearing in Table 7. Furthermore, the formation of HXeCN is accompanied with the efficient formation of HXeNC with the strong bands at 1850.9 and 2044.0 cm^{-1}, and these do not appear in the experiments with cyanoacetylene. Based on these arguments, we rule out the formation of HKrCN and HXeCN as major species in the present experiments with cyanoacetylene.

The motivation of our computations on the Kr···HKrCCCN and Kr···HKrCCNC complexes comes from the fact that the noble gas molecules are experimentally studied in solid matrix, whereas the computations refer to vacuum. The consideration of the 1:1 complexes gives ideas about the interaction strength of the embedded molecules with matrix atoms and the influence of this interaction on the vibrational spectrum. It was previously suggested that such specific interactions are relevant to the experimentally observed matrix site band structure of noble gas hydrides.[36] For Kr···HKrCCCN, the computational splitting of the H−Kr stretching bands produced by different 1:1 complex geometries is about 40 cm^{-1}, and the experimental bands are split at least by 20 cm^{-1}. Other computational bands (ω_1 and ω_3 modes) are affected by complexation less extensively, which is in agreement with the experiment. Thermal modification of the HKrCCCN bands observed after annealing at 40 K in a Kr matrix confirms the assignment of the band splitting to the matrix site effect and establishes some correspondence between the matrix site bands in different spectral regions. Despite the good qualitative agreement between experiment and theory for the 1:1 complexes observed also previously,[36] the situation is not so simple, and multiple interactions should be considered to reach a more adequate description. In ref 23, the matrix site structure of $HNgC_4H$ was explained by perturbation of its linear structure when embedded in a solid matrix, and this speculation is relevant to the present case as well. The direct simulation of an HNgY molecule in a solid matrix is a very complicated computational task.[58]

Annealing of the photolyzed HCCCN/Ar matrixes produced no bands that can be assigned to HArCCCN. It is not absolutely clear why this product is not formed in these experiments although it is computationally stable; however, several probable reasons exist and can be commented on. First, some overestimate of the energetic stability with respect to the H + Ar + CCCN asymptote is probable because the calculation of the energy of CCCN may be somewhat inaccurate with the single-reference MP2 computational method. Second, the H + Ar + CCCN reaction can be protected with an energy barrier, which is essential at the relatively low annealing temperature used in an Ar matrix. Finally, the competing reaction channels leading to HCCCN and HNCCC can dominate over the formation of HArCCCN.

Decay of $KrHKr^+$ and Tentative Assignment of CCCN Radical. One experiment should be discussed in more detail. After photolysis of an HCCCN/Kr matrix, the spectra show strong absorption bands of $KrHKr^+$. It is well-known that these cations decay with time even at very low temperatures.[59,60] We studied the effect of the cations on the annealing-induced formation of the noble gas hydrides and possible formation of some species upon neutralization of the cations. After ∼20 h at 8 K, practically no presence of cations is seen in the absorption spectra. No formation of $HKrC_3N$ was observed at low temperatures. Upon subsequent annealing at 30 K, the $HKrC_3N$ formation was observed in amounts similar to the experiments without the long preannealing period. This observation supports that the ionic channels do not participate efficiently in the formation of $HKrC_3N$, as was previously discussed for other noble gas hydrides.[15,23,57,61,62] In this experimentally approved model, the formation of HNgY molecules generally occurs in the H + Ng + Y reaction of the neutral fragments.

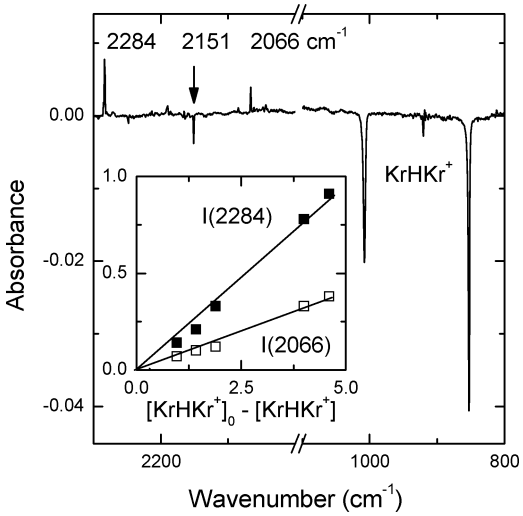

Figure 6. Difference spectrum showing the result of relaxation of matrix species for 20 h at 8 K. The $NC_3{}^{15}N$/Kr sample was first photolyzed with the 193 nm radiation. The increasing bands at 2284 and 2066 cm^{-1} are tentatively assigned to $CCC^{15}N$ radical, and the decreasing band at 2151 cm^{-1} is probably from $CCC^{15}N^-$. The inset shows the correlation of the 2284 and 2066 cm^{-1} bands with the decrease of the relative $KrHKr^+$ concentration as compared with the initial concentration obtained after 193 nm photolysis. The data points in the inset correspond to different relaxation periods.

The second result of this experiment deserves further discussion. Upon the slow decay of $KrHKr^+$, we observed a synchronous increase of two bands at 2284 and 2066 cm^{-1} and a decrease of a band at 2151 cm^{-1} (see Figure 6 for the experiment with ^{15}N-cyanoacetylene in a Kr matrix). The two rising bands agree with the computational vibrational spectrum of the CCCN radical. McCarthy et al. reported computational bands of $CCC^{14}N$ radical at 2311.8 and 2116.6 cm^{-1}.[32] The experimental bands obtained from $HCCC^{14}N$ are at 2298 and 2076 cm^{-1} in a Kr matrix and at 2303 and 2079 cm^{-1} in an Ar matrix, which is a good agreement with the results by McCarthy et al. and shows the proper isotope shift. The band at 2151 cm^{-1} in a $HCCC^{15}N$/Kr matrix probably belongs to one matrix site of $CCCN^-$. It is probable that this matrix site of $CCCN^-$ is determined by the presence of $KrHKr^+$ in the close proximity. In many experiments, the decomposition of the $HNgC_3N$ hydrides by light produces these bands tentatively assigned to CCCN and C_3N^-, which would be natural decomposition channels together with HCCCN.

The assignment of the bands at 2284 and 2066 cm^{-1} to $CCC^{15}N$ would lead to one interesting consequence. In this case, the formation of CCCN occurs at least partially upon neutralization of $KrHKr^+$ and $CCCN^-$. The neutralization of these ionic species does not involve global mobility of protons in the matrix because no hydrogen-containing species are built up and other negative ions present in the matrix (C_2NC^-, C_2N^-, CN^-) do

not decay together with $KrHKr^+$. We have suggested recently that the decay of these cations is a local process involving a movement of an electron from an electronegative fragment to the solvated proton,[60,63] which is a consequence of locality of photolysis in noble gas matrixes.[64] Our present results are consistent with this model.

Other Products: Any Candidates for HCCNgCN and HCCNgNC? Upon photolysis and annealing of HCCCN/Ng samples, many channels are possible for various closed-shell, open-shell, neutral, and positively and negatively charged products, and we discuss some of them. The bands at 1792 and 901 cm^{-1} in an Ar matrix were assigned in the literature to the bent CCNC radical.[30] At the level of theory used in ref 30, this is a quartet (excited) state radical, which is about 2.7 eV higher in energy than the quasi-linear ground-state structure (see Table 4). Our calculations for the bent $CC^{14}NC$ radical give the strongest bands at 1856.7 and 935.5 cm^{-1}, in agreement with experiment. Upon ^{15}N isotope substitution, these bands shift to 1789 and 893 cm^{-1} in an Ar matrix, i.e., the experimental $^{15}N/^{14}N$ isotope shifts are quite minor (-3 and -8 cm^{-1}). The computational shifts of these bands upon ^{15}N substitution are -33 and -4 cm^{-1}, hence featuring a poor agreement with the experimental value for the strongest band. In addition, a disagreement between experiment and calculations are observed for the band at 2087 cm^{-1} in a Kr matrix, which is assigned following ref 30 to $CCNC^-$. According to our calculations, the ^{15}N-induced shift is -25 cm^{-1}, whereas -2 cm^{-1} is found in experiment. These assignments seem to need further justification.

The band at 2023 cm^{-1} in an Ar matrix was assigned by Guennoun et al. to CN^-.[30] Upon ^{15}N isotope substitution, this band is at 1987 cm^{-1}, i.e., it shifts down in energy by -36 cm^{-1}. This shift is too large for a two atomic species even in the harmonic approximation using the reduced masses, which yields the -31.5 cm^{-1} downshift. Our ab initio calculations on CN^- give a shift of -30.3 cm^{-1} (see Table 4). Furthermore, the computational absorption intensity of this band (<3 km/mol) is very low, whereas the experimental band (2023 cm^{-1} in an Ar matrix) is strong. This consideration brings some doubts about the assignment of this band to isolated CN^-. Another candidate to consider is the ground-state CCNC radical (^2D) with a computational frequency of 2064.0 cm^{-1} and ^{15}N isotope shift of -37.2 cm^{-1}, which would agree well with the experimental value. A complication with this assignment concerns the computational band at 1720.4 cm^{-1}, which should also be strong enough for experimental observation but not seen in the spectra. Another strong experimental band at 1461 cm^{-1} seems to correlate with the 2023 cm^{-1} band, but it is not predicted at the level of theory used here. These two bands (2023 and 1461 cm^{-1}) are efficiently decomposed by irradiation at 488 nm from an Ar-ion laser, and some formation of the bands assigned to the bent CCNC radical simultaneously takes place. The 1461 cm^{-1} band might belong to some unidentified species. It is also possible that these bands originate from another structure of CCNC with spectroscopic features of CC^+ and CN^-. Interestingly, photolysis in a Xe matrix does not produce some of the bands present in Ar and Kr matrixes. In particular, this concerns the bands assigned previously to CN^- and the bent CCNC radical. Examples are known when photolysis products differ greatly in experiments in a Xe matrix from other solid hosts.[65]

In our experiments, no strong candidates for HCCNgCN and HCCNgNC molecules are seen. In principle, the formation of these species is possible because the HCC + CN channel is known for 193 nm photolysis of cyanoacetylene in the gas phase.[27] In solid matrixes, the formation of these noble gas compounds would mean an exchange of positions of one matrix atom with either HCC or CN, which is not impossible.[51] The only suitable absorption found in the spectra is the 2023 cm^{-1} band in an Ar matrix, previously assigned to CN^-.[30] This band would correspond to the strongest ω_2 mode of HCCArCN or HCCArNC which is computationally at 2023.7 and 1997.4 cm^{-1}, respectively (see Table 1). The experimental ^{15}N shift for this band is -36 cm^{-1}, and it is computationally -29.3 cm^{-1} for HCCArCN and -31.7 cm^{-1} for HCCArNC. Upon deuteration, these bands are practically unchanged, which is suitable for this assignment. However, the problem with the accompanying band at 1461 cm^{-1} still exists. Moreover, for Ng = Kr, the corresponding band for a similar noble gas compound computationally shifts to a higher energy as compared to Ng = Ar (see Table 1), whereas the experiment gives a small red shift, which is more suitable for a normal matrix effect. In any case, the confident assignment of such noble gas compound is a very complicated task because of the absence of the characteristic H−Ng stretching mode. The bands involving a Ng atom are at relatively low energy (computationally 482 cm^{-1} with the intensity of 117 km/mol for HCCArCN and 347 cm^{-1} with the intensity of 776 km/mol for HCCArNC).

Additional possible products are worth mentioning. The $CCHCN^-$ and $CCHNC^-$ radical anions can be formed during photolysis similarly to the known matrix-isolated species $BrHBr^-$, $ClHCl^-$, etc.[66] Upon annealing, the H + HC_3N reaction (with various isomers) can lead to a number of H_2C_3N species similarly to the known reactions H + HCN and H + HNCO.[57,67] The reaction with the precursor is probable because the complete photodecomposition of the precursor is complicated by the known self-limitation of solid-state photolysis.[68] These hypothetical but probable channels complicate the analysis of numerous weak bands present in the experimental spectra.

Concluding Remarks

The insertion of noble gas atoms into cyanoacetylene (HCCCN) has been studied. A number of novel noble gas insertion compounds are investigated computationally, and their kinetic stability is found at the MP2/6-311++G(*2d*,*2p*) level of theory. The first group of novel molecules belongs to noble gas hydrides (HNgCCCN and HNgCCNC), and we found their computational stability for Ng = Ar, Kr, and Xe. The strong H−Ng stretching absorption makes their experimental detection relatively easy and reliable. The HNgCCCN compounds with Kr and Xe are similarly stable as previously identified HKrCN and HXeCN.[57] The HArCCCN molecule seems to be less stable than the previously identified HArF molecule.[5,17,18] The HNgCCNC molecules are computationally less stable than the HNgCCCN isomers for all the noble gas atoms (Ar, Kr, Xe). The second group of the computational insertion compounds are of a different type, HCCNgCN and HCCNgNC, and they are kinetically stable for Ng = Ar, Kr, and Xe. All these compounds are charge-transfer molecules with a positive charge localized in a large part at the noble gas atom. To our knowledge, the HCCArNC molecule represents the first computational result on the stable Ar−N bond in a neutral compound.

The experiments with low-temperature cyanoacetylene/Ng (Ng = Ar, Kr, and Xe) matrixes evidence the formation of two noble gas hydrides for Ng = Kr and Xe, with the strongest H−Ng stretching absorption bands at 1492.1 and 1624.5 cm^{-1}, respectively. The computational spectra of HKrCCCN and

HXeCCCN agree better with the experimental data, whereas the HNgCCNC isomers are less probable. The obtained species absorb at similar frequencies to the HKrCN and HXeCN molecules,[57] which is in agreement with the theoretical predictions. No strong candidates for an Ar compound are observed although the case is still open, at least for the HCCArNC and HCCArCN species.

Photolysis and annealing of cyanoacetylene in noble gas matrix produces numerous closed-shell, open-shell, neutral, and charged products. A number of bands are unidentified so far. Furthermore, some of the literature assignments seem to need further justification, as suggested by the comparison of our experimental and computational data on the ^{15}N-labeled species, for instance, for CN^-, $CCNC^-$, and bent CCNC radical. On the other hand, this disagreement might be caused by possible inaccuracy of the conventional computational methods used here. The results obtained in long-term decay of $KrHKr^+$ cations suggest a tentative assignment for CCCN radical (bands at 2284 and 2066 cm^{-1} for ^{15}N-labeled species in a Kr matrix).

Acknowledgment. The Academy of Finland supported this work. Zohra Guennoun and Peter Botschwina are thanked for the valuable information. CSC is acknowledged for the computational resources.

References and Notes

(1) Bartlett, N. *Proc. Chem. Soc.* **1962**, 218.
(2) Brel, V. K.; Pirkuliev, N. S.; Zefirov, N. S. *Russ. Chem. Rev.* **2001**, *70*, 231.
(3) Turner, J. J.; Pimentel, G. C. *Science* **1963**, *140*, 974.
(4) Lehman, J. F.; Mercier, H. P. A.; Schrobilgen, G. J. *Coord. Chem. Rev.* **2002**, *233*−*234*, 1.
(5) Khriachtchev, L.; Pettersson, M.; Runeberg, N.; Lundell, J.; Räsänen, M. *Nature* **2000**, *406*, 874.
(6) Wang, M. W. *J. Am. Chem. Soc.* **2000**, *122*, 6289.
(7) Takayanagi, T.; Wada, A. *Chem. Phys. Lett.* **2002**, *352*, 91.
(8) Bihary, Z.; Chaban, G. M.; Gerber, R. B. *J. Chem. Phys.* **2002**, *117*, 5105.
(9) Lignell, A.; Khriachtchev, L.; Pettersson, M.; Räsänen, M. *Chem. Phys. Lett.* **2004**, *390*, 256.
(10) Khriachtchev, L.; Pettersson, M.; Lundell, J.; Tanskanen, H.; Kiviniemi, T.; Runeberg, N.; Räsänen, M. *J. Am. Chem. Soc.* **2003**, *125*, 1454.
(11) Cohen, A.; Lundell, J.; Gerber, R. B. *J. Chem. Phys.* **2003**, *119*, 6415.
(12) Lundell, J.; Panek, J.; Latajka, Z. *Chem. Phys. Lett.* **2001**, *348*, 147.
(13) Ghanty, T. K. *J. Chem. Phys.* **2006**, *124*, 124304.
(14) Lundell, J.; Khriachtchev, L.; Pettersson, M.; Räsänen, M. *Low Temp. Phys.* **2000**, *26*, 680.
(15) Pettersson, M.; Khriachtchev, L.; Lundell, J.; Räsänen, M. Noble Gas Hydride Compounds. In *Inorganic Chemistry in Focus II*; Meyer, G., Naumann, D., Wesemann, L., Eds.; Wiley-VCH: Weinheim, Germany, 2005; pp 15−34.
(16) Pettersson, M.; Lundell, J.; Räsänen, M. *J. Chem. Phys.* **1995**, *102*, 6423.
(17) Khriachtchev, L.; Pettersson, M.; Lignell, A.; Räsänen, M. *J. Am. Chem. Soc.* **2001**, *123*, 8610.
(18) Khriachtchev, L.; Lignell, A.; Räsänen, M. *J. Chem. Phys.* **2004**, *120*, 3353.
(19) Pettersson, M.; Khriachtchev, L.; Lignell, A.; Räsänen, M.; Bihary, Z.; Gerber, R. B. *J. Chem. Phys.* **2002**, *116*, 2508.
(20) Khriachtchev, L.; Tanskanen, H.; Lundell, J.; Pettersson, M.; Kiljunen, H.; Räsänen, M. *J. Am. Chem. Soc.* **2003**, *125*, 4696.
(21) Feldman, V. I.; Sukhov, F. F.; Orlov, A. Yu.; Tyulpina, I. V. *J. Am. Chem. Soc.* **2003**, *125*, 4698.
(22) Khriachtchev, L.; Tanskanen, H.; Cohen, A.; Gerber, R. B.; Lundell, J.; Pettersson, M.; Kiljunen, H.; Räsänen, M. *J. Am. Chem. Soc.* **2003**, *125*, 6876.
(23) Tanskanen, H.; Khriachtchev, L.; Lundell, J.; Kiljunen, H.; Räsänen, M. *J. Am. Chem. Soc.* **2003**, *125*, 16361.
(24) Tanskanen, H.; Khriachtchev, L.; Lundell, J.; Räsänen, M. *J. Chem. Phys.* **2004**, *121*, 8291.
(25) Baumfalk, R.; Nahler, N. H.; Buck, U. *J. Chem. Phys.* **2001**, *114*, 4755.
(26) Nahler, N. H.; Farnik, M.; Buck, U. *Chem. Phys.* **2004**, *301*, 173.
(27) Seki, K.; He, M.; Liu, R.; Okabe, H. *J. Phys. Chem.* **1996**, *100*, 5346.
(28) Kolos, R.; Waluk, J. *J. Mol. Struct.* **1997**, *408*−*409*, 473.
(29) Titarchuk, T.; Halpern, J. B. *Chem. Phys. Lett.* **2000**, *323*, 305.
(30) Guennoun, Z.; Couturier-Tamburelli, I.; Pietri, N.; Aycard, J. P. *Chem. Phys. Lett.* **2003**, *368*, 574.
(31) Botschwina, P. *Phys. Chem. Chem. Phys.* **2003**, *5*, 3337.
(32) McCarthy, M.; Gottlieb, C. A.; Thaddeus, P.; Horn, M.; Botschwina, P. *J. Chem. Phys.* **1995**, *103*, 7820.
(33) The computations are performed with: *Gaussian03*, revision B.02; Gaussian, Inc.: Pittsburgh, PA, 2003.
(34) Runeberg, N.; Pyykkö, P. *Int. J. Quantum Chem.* **1988**, *66*, 131.
(35) Lignell, A.; Khriachtchev, L.; Pettersson, M.; Räsänen, M. *J. Chem. Phys.* **2003**, *118*, 11120.
(36) Khriachtchev, L.; Lignell, A.; Juselius, J.; Räsänen, M.; Savchenko, E. *J. Chem. Phys.* **2005**, *122*, 014510.
(37) Jung, J. O.; Gerber, R. B. *J. Chem. Phys.* **1996**, *105*, 10332.
(38) Jung, J. O.; Gerber, R. B. *J. Chem. Phys.* **1996**, *105*, 10682.
(39) Chaban, G. M.; Jung, J. O.; Gerber, R. B. *J. Chem. Phys.* **1999**, *111*, 1823.
(40) Chaban, G. M.; Jung, J. O.; Gerber, R. B. *J. Phys. Chem. A* **2000**, *104*, 2772.
(41) Matsunagi, N.; Chaban, G. M.; Gerber, R. B. *J. Chem. Phys.* **2002**, *117*, 3541.
(42) Schmidt, M. W.; Baldridge, K. K.; Boatz, J. A.; Elbert, S. T.; Gordon, M. S.; Jensen, J. H.; Koseki, S.; Matsunaga, N.; Nguyen, K. A.; Su, S. J.; Windus, T. L.; Dupuis, M.; Montgomery, J. A. *J. Comput. Chem.* **1993**, *14*, 1347.
(43) Basis sets were obtained from the Extensible Computational Chemistry Environment Basis Set database, version 02/25/04, as developed and distributed by the Molecular Science Computing Facility, Environmental and Molecular Sciences Laboratory, which is part of the Pacific Northwest Laboratory, P.O. Box 999, Richland, WA 99352 U.S.A. and funded by the U.S. Department of Energy. The Pacific Northwest Laboratory is a multiprogram laboratory operated by Battelle Memorial Institute for the U.S. Department of Energy under contract DE-AC06-76RLO 1830. Contact Karen Schuchardt for further information.
(44) Lundell, J.; Pettersson, M.; Khriachtchev, L.; Räsänen, M.; Chaban, G. M.; Gerber, R. B. *Chem. Phys. Lett.* **2000**, *322*, 389.
(45) Khriachtchev, L.; Lundell, J.; Pettersson, M.; Tanskanen, H.; Räsänen, M. *J. Chem. Phys.* **2002**, *116*, 4758.
(46) Li, S.; Cohen, A.; Gerber, R. B. *J. Am. Chem. Soc.* **2006**, *128*, 7156.
(47) Nemukhin, A. V.; Grigorenko, B. L.; Khriachtchev, L.; Tanskanen, H.; Pettersson, M.; Räsänen, M. *J. Am. Chem. Soc.* **2002**, *124*, 10706.
(48) McDowell, S. A. C. *Phys. Chem. Chem. Phys.* **2003**, *5*, 808.
(49) Melamed, U.; Feit, B. A. *J. Org. Chem.* **1983**, *48*, 1928.
(50) Hay, L. A.; Koenig, T. M.; Ginah, F. O.; Copp, J. D.; Mitchell, D. *J. Org. Chem.* **1998**, *63*, 5050.
(51) Apkarian, V. A.; Schwentner, N. *Chem. Rev.* **1999**, *99*, 1481.
(52) Eberlein, J.; Creuzburg, M. *J. Chem. Phys.* **1997**, *106*, 2188.
(53) Khriachtchev, L.; Tanskanen, H.; Pettersson, M.; Räsänen, M.; Feldman, V.; Sukhov, F.; Orlov, A.; Shestakov, A. F. *J. Chem. Phys.* **2002**, *116*, 5708.
(54) Khriachtchev, L.; Saarelainen, M.; Pettersson, M.; Räsänen, M. *J. Chem. Phys.* **2003**, *118*, 6403.
(55) Ahokas, J.; Kunttu, H.; Khriachtchev, L.; Pettersson, M.; Räsänen, M. *J. Phys. Chem. A* **2002**, *106*, 7743.
(56) Khriachtchev, L.; Tanskanen, H.; Pettersson, M.; Räsänen, M.; Ahokas, J.; Kunttu, H.; Feldman, V. *J. Chem. Phys.* **2002**, *116*, 5649.
(57) Pettersson, M.; Lundell, J.; Khriachtchev, L.; Räsänen, M. *J. Chem. Phys.* **1998**, *109*, 618.
(58) Bochenkova, A. V.; Firsov, D. A.; Nemukhin, A. *Chem. Phys. Lett.* **2005**, *405*, 165.
(59) Bondybey, V. E.; Pimentel, G. C. *J. Chem. Phys.* **1972**, *56*, 3832.
(60) Khriachtchev, L.; Lignell, A.; Räsänen, M. *J. Chem. Phys.* **2005**, *123*, 064507.
(61) Pettersson, M.; Nieminen, J.; Khriachtchev, L.; Räsänen, M. *J. Chem. Phys.* **1997**, *107*, 8423.
(62) Khriachtchev, L.; Tanskanen, H.; Räsänen, M. *J. Chem. Phys.* **2006**, *124*, 181101.
(63) Lignell, A.; Khriachtchev, L.; Lignell, H.; Räsänen, M. *Phys. Chem. Chem. Phys.* **2006**, *8*, 2457.
(64) Khriachtchev, L.; Pettersson, M.; Lundell, J.; Räsänen, M. *J. Chem. Phys.* **2001**, *114*, 7727.
(65) Khriachtchev, L.; Pettersson, M.; Jolkkonen, S.; Pekkonen, S.; Räsänen, M. *J. Chem. Phys.* **2000**, *112*, 2187.
(66) Räsänen, M.; Seetula, J.; Kunttu, H. *J. Chem. Phys.* **1993**, *98*, 3914.
(67) Pettersson, M.; Khriachtchev, L.; Jolkkonen, S.; Räsänen, M. *J. Phys. Chem. A* **1999**, *103*, 9154.
(68) Khriachtchev, L.; Pettersson, M.; Räsänen, M. *Chem. Phys. Lett.* **1998**, *288*, 727.